Transactions of the 15th International Conference on
Structural Mechanics in Reactor Technology (SMiRT-15)
Seoul, Korea, August 15-20, 1999

Coupled Thermo-Hydraulic and Elastic-Plastic Analyses of a Cracked Inclined Nozzle

Ph. Gilles[1], C. Bois[1], A. Woaye Hune[1] and G. Bezdikian[2]

1) FRAMATOME, France
2) EDF/EPN, France

ABSTRACT

EDF and FRAMATOME have conducted an important programme on the fracture behavior of aged duplex cast stainless steel components. This paper presents two fracture analyses on a 45° lateral nozzle under hydrotest pressure and thermo-mechanical loadings respectively . The paper gives first an overview of the different steps of these analyses, then a comparison between defect assessment under these two loading conditions. The study has two original features : the thermal transient is obtained from a thermo-hydraulic calculation of the turbulent flow in the nozzle and meshes of the cracked nozzle are generated automatically using a modelling system developed for cracked structures by SYSTUS – International and FRAMATOME. It is concluded that for the defects postulated at the most severe location, there is no tearing initiation even after 40 year ageing of the material.

1. INTRODUCTION

Piping cast components made of duplex stainless steel contain small shrinkage cavities due to the manufacturing process and are susceptible to thermal ageing embrittlement. Therefore, EDF and FRAMATOME have developed a large research Program on the evolution of in-service component mechanical properties, on the detection of cavities, on fracture behavior of large scale structures and on defect assessment ([1] to [4]). The present study analyses the tearing initiation resistance of the nozzle connecting the Safety Injection System to the cold leg of the Main Coolant Line in a 1300 MWe Pressurised Water Reactor.

1.1. Objective of the Study

Since non-destructive examinations are more difficult to conduct in a nozzle, the objective of the fracture assessments is to analyse envelope cracks of potential defects centred at the most severe location. This study aims at determining these cracks under the most severe loading conditions (hydrotest and safety injection) and at verifying that, in spite of the decrease of tearing resistance due to thermal ageing, no risk of initiation is to be feared.

In order to avoid the conservatism of usual thermal computations, a 3D thermo-hydraulic calculation of the nozzle and the turbulent water is conducted using the STAR CD software [5]. The envelope cracks are located on the basis of the largest normal stress. Two configurations are obtained, both centred in the symmetry plane : a nozzle with a corner crack and a nozzle with a crack located on the inner wall of the branch, close to the corner. We refer to them as corner crack and branch crack geometries.

1.2. Main Data of the Mechanical Analysis

The structure is an 45°-inclined nozzle connecting two circular cylinders. The inner diameter and thickness of the run are respectively 700 and 66 mm. For the branch, these dimensions are 222.2 and 25.4 mm. After manufacturing, all the cast components are subjected to extensive non-destructive examinations. The results relative to 60 nozzles show reveal a low number of shrinkage cavities. Dye penetrant inspections are used to detect surface defects. The largest ones are repaired and their depth varies mostly between 2 and 7 mm. Since defects are smaller and less numerous on the inner wall, the depth of the envelope defects has been fixed to 10 mm. Their location and size are given in Table 2.

The nozzle is made of Z3 CND 19-10 M duplex stainless steel. End-of-life values of the heat which is the most sensitive to thermal ageing have been chosen for the thermo-mechanical characteristics. These characteristics are considered as temperature independent, but two different sets of values have been chosen for each of the two loading cases. For the hydrotest, tensile properties are taken at the test temperature. For the safety injection transient condition, the temperature has been chosen to maximise the crack driving force at the deepest point. Poisson's ratio is 0.3. The selected material characteristic values are reported in table 1.

Table 1: Material characteristics for the elasto-plastic computations

Loading condition	Temperature (°C)	Young Modulus (MPa)	Yield stress (MPa)	10% ε_t stress (MPa)	Thermal Expansion Coefficient ($°C^{-1}$)
Hydrotest	100	184800	218	441	-
Nominal pressure + Safety Injection	227.5	180500	175	379	$17.3\ 10^{-6}$

For 1300 MWe reactors, the minimum value of the end-of-life toughness of the duplex stainless steel nozzles has been estimated to 68 kJ/m^2 at 100°C. This value is about 25% lower for 900 MWe nozzles.

The hydrotest loading is represented by a pure pressure increase from 0 to 20.7 MPa. The safety injection loading contains two-steps. First pressure and temperature are increasing together respectively from 0 to 12.9 MPa and from 0 to 297°C. In a second step, an instantaneous thermal shock is applied in the branch pipe from 297 to 0°C, under a constant pressure of 12.9 MPa.

2. THERMO-HYDRAULIC CALCULATION OF THE HEAT TRANSFER FROM TURBULENT WATER TO NOZZLE

For thick components such as a nozzle on the Main Coolant Line, thermal shocks give rise to large stress values. Therefore, improving the accuracy of the temperature computation in the nozzle under thermal transients, is of peculiar importance.

In the usual approach, temperature distributions in the fluid and in the structure are estimated separately. Thermal computations in the structure requires the determination of heat exchange coefficients along the inner wall at various temperatures. This determination is based on experimental measurements on a mock-up and conservative extrapolations. Since measurements were available only on T joints, the margins would have been larger, leading to over-estimate the risk of crack initiation under thermal loading. It was then decided to perform a 3D coupled thermo-hydraulic and thermo-mechanical calculation of the inclined nozzle.

The initial state corresponds to the nominal flow in the primary leg under which a uniform temperature distribution of 297°C is assumed in the nozzle. The thermal loading consists in an auxiliary pipe inflow of cold water (10°C) with a time dependant flow rate over 240 seconds, followed by a hot shock induced by the end of the cold inflow. The different steps of the thermal-hydraulic calculations are detailed below:

- Preliminary axi-symmetrical calculations are performed on the branch to account for the cold shock attenuation due to the presence of the hot dead leg (initially at a nominal temperature of 297°C on a distance of 13 times the auxiliary pipe inside diameter). The results obtained at the outlet of this model are used to define the transient fluid temperatures and characteristics at the inlet of the 3D nozzle model.,
- 3D thermo-hydraulic permanent calculation on the nozzle to define the initial conditions before the safety water injection,
- 3D thermo-hydraulic transient calculation to evaluate the continuous time and space temperature distributions over the whole nozzle, during and after the cold fluid water safety injection. The inlet variable flow rates in the nozzle are those issued from the 2D approach presented above.

All the thermo-hydraulic calculations are performed using the general computational fluid dynamic software STAR-CD [5] which incorporates a numerical finite volume procedure for solving the governing differential conservation equations of mass, momentum and energy of laminar or turbulent flows. In the latter case, the effects of turbulence are represented by the additional equations of a model coupling kinetic energy K and dissipation energy rate ε. A special attention is paid to the modelisation of the actual tangential velocity profile inside the boundary layers. The velocity profile is assessed with an algebraic formula called "wall function" which connects the evolution of the tangential velocity to the normalised distance from the wall (Y+). Y+ is given by the following equation:

$$Y+ = \frac{\rho}{\mu} y \frac{U}{4 + 6\log_{10} Y+} \qquad (1)$$

where ρ is the fluid density (kg/m^3), μ the laminar dynamic viscosity (Pa.s), y the thickness of the mesh near the wall (m) and U the mean velocity (m/s).

The wall function is valid and gives good results when the value of Y+ is within the range of [30 ,2000]. The first layers of the mesh near the inner wall have been sized to satisfy this requirement as much as possible, ensuring a good accuracy of the temperature distributions inside the fluid and the solid. The mesh contains about 61800 fluid and 30200 solid elements. Thermal gradients in the corner zone are shown on Figure 1.

3. SELECTION OF THE MOST SEVERE CRACK LOCATIONS

Under combined pressure and thermal transient, the determination of the most severe location with respect to crack initiation is based on thermo-mechanical elastic computations on the sound nozzle. The Finite Element method is used for stress computations, requiring a quite different mesh as in Finite Volume computations. The refinement has to be increased in potential stress concentration zones such as the two-pipe intersection, but not along the inner wall. The elements are second order isoparametric prisms or cubes. Therefore the temperature distributions at the nodes of the mechanical mesh, have been again calculated with SYSTUS+ [6] from the inner wall temperatures obtained with STAR-CD. Crack initiation under dominant thermal loading depends mainly on the value of the stress normal to the crack plane. In order to select the zones of maximum crack opening stresses, the following two step procedures is applied.

First, thermal instants susceptible to induce large stresses in the structure are selected using two parameters ΔT1 and ΔT2 defining the temperature variation through the thickness. ΔT1 is the linear thermal gradient, and ΔT2 the second order coefficient. The variations of these parameters are analysed along 70 segments shown on Figure 2. For each of these wall cross sections, the ΔT1 and ΔT2 variations are quite similar: ΔT2 reach a maximum between 50 to 100 seconds, and ΔT1 between 200 to 250s. 12 instants are selected for which the elastic stress distributions are computed in the nozzle.

In a second step, these thermal stresses are combined with stresses in the elastic nozzle under hydrotest pressure. In each of the wall cross sections, maximal principal stress values are determined. The postulated defect is centred at the point corresponding to the largest principal stress in the plane normal to the associated direction. The most severe crack is located in the symmetry plane, along the inner wall of the branch but very close to the corner of the nozzle intersection as shown on Figure 2 between segment 1 and 2.

Under pure pressure, the most severe crack is also in the plane of symmetry, centred at the corner. Locations and sizes of the two cracks are summarised in Table 2.

Table 2: Geometrical characteristics of the selected defects

Pipe	Notch Location	Notch Orientation	Length 2c (mm)	Depth a (mm)	c/a
RUN	Symmetry plane Corner	Longitudinal	210	10	1
BRANCH	Symmetry Plane Close to the corner	Longitudinal		10	2

4. BEHAVIOR OF THE NOZZLE WITH A CORNER CRACK

The two meshes of the cracked configurations are obtained using special processors of the SYSTUS code [6] allowing generation of the mesh of the sound nozzle and insertion of a cracked block of elements in this mesh (Fig. 3). These tools automatically give a large set of detailed results relative to the crack behavior. The meshes contain about 12000 nodes and 2400 quadratic prismatic and cubic elements. The nozzle contains 5 elements in the thickness. Branch and run cylinders have been lengthened to avoid end effects on the results. All the computations are performed under the small displacement hypothesis.

A detailed analysis of the corner crack is performed for mesh validation purpose. The crack driving force J is computed via the G-θ domain integral method [7]. The results θJ. are compared to Stress Intensity Factor values determined from crack tip opening displacements, and to those obtained using the CETIM influence functions [8]. Symmetry conditions explain the pure mode I behavior of the crack. Under pure pressure, SIF results give J estimates 8% lower than θJ except at the edge points where SIF values are underestimated. The SIF obtained with the influence functions correspond to lower J values except at the edge points where they are 10% higher than θJ. The same trends are observed under the second loading, however the third order influence functions are less accurate for thermo-mechanical loads for which stress distributions are less regular. The observed differences are quite acceptable, since the two SIF estimation methods are always less accurate than the G-θ method.

At the end of the hydrotest, the elasto-plastic computation reveals that the nozzle remains mainly elastic: as shown on Figure 4, yielding is contained in the corner area. The J variations along the crack front are similar to the elastically computed ones Je. The ratio J/Je is 1.15 along the main part of the crack, but becomes lower than unity at the edge points (0.89).

5. BEHAVIOR OF THE NOZZLE WITH A CRACK LOCATED IN THE BRANCH

For each instant of the transient, temperatures in the nozzle are applied on the cracked mesh during the elastic-plastic computations. Elastic computations are performed mostly to estimate the stress relaxation under thermo-mechanical loading. As for the corner crack, θJ values are higher than those deduced from SIF obtained from crack tip opening displacements in the two loading cases. Under pure pressure, the J distribution along the crack front is not symmetrical as for the corner crack: J values are much higher on the MCL side. Under combined pressure (12.9 MPa) and cold shock, the J distribution along the crack front is almost symmetrical.

The elasto-plastic analysis under pressure shows, as for the corner crack case, that yielding is concentrated in the corner area. A small plastic zone follows the crack front: the J values are 40 to 50% larger than the elastic values Je, except on the MCL side where J and Je values are almost identical. Under combined pressure and thermal shock, yielding is concentrated along the branch inner wall. The thermal load acts opens more the edges than the deepest point, and J tends to become uniform along the crack front with increasing load. The stability of the J values with respect to the domain of J-integration is perfectly verified at each load step. At the end of the shock, J values are 30 to 50% lower than in the elastic case.

The behaviours of the two cracks under the two loading cases are compared using the Crack Mouth Openings. Figures 5a and 5b show that for the corner crack, the pressure load leads to the largest opening and for the branch crack, the thermo-mechanical load gives the envelope opening results. This validates the procedure of selection of the worst location for the postulated crack under a given load.

Table 3 summarises the maximum J values, showing that the safety injection transient is more severe than the hydrotest and that the most severe crack does not initiate.

Table 3: Maximum J values (kJ/m^2).

Loading case	Corner Crack	Branch Crack	$J_{0.2}$ (100 °C)
Hydrotest Pressure	31	23	68
Safety Injection	31	40.5	68

6. CONCLUSIONS

The main advantage of the coupled thermo-hydraulic approach for the thermal computation is the availability of the continuous temperature distribution in the fluid as well as in the structure and for any time of the transient. For complex structures, this approach is much more reliable than the classical method based on an empirically fitted exchange coefficient.

The comparison of the opening behaviours of the two cracks under the two types of loading, show that the centre and branch cracks were centred at the most severe location respectively for hydrotest and safety injection conditions. In both cases, the maximum J value remains lower to a conservative estimate of the tearing resistance.

7. REFERENCES

1. Bezdikian, G., Churier-Bossenec, H., et al., "Life Evaluation of Cast Stainless Elbows on PWR primary circuit", *Proc. Of the 5th International Conference on Nuclear Engineering, ICÔNE-2490*, Nice France, May 1997.

2. Le Delliou, P. and Sémété, P. ,"Large Scale Tests on Aged Cast Duplex Stainless Steel Elbows : Results and Lessons Drawn", *Proc. Of the 7th International Conference on Nuclear Engineering, ICÔNE-7114,* Tokyo Japan, April 1999.

3. Massoud, J. P., Jayet-Gendrot, S. et al., "Thermal Ageing of Cast Duplex Stainless Steel Primary Components. Overview of the Research Programme Conducted by EDF", *Proc. Of the 5th International Conference on Nuclear Engineering, ICÔNE-2497*, Nice France, May 1997.

4. Gilles, Ph., Bois, C., Le Delliou P., "Numerical and simplified analyses of large scale ductile tearing tests on cracked elbows", *Proc. Of the 14th SMIRT Conference*, Lyon France, August 1997.

5. Code STAR-CD. Version 2.21. Distributed by ADAPCO, Paris-La-Défense France.

6. Code SYSTUS. Version 233 19/04/1996. SYSTUS International, 69485 Lyon France.

7. Destuynder Ph., Djaoua M. 1981. Sur une interprétation mathématique de l'intégrale de Rice en théorie de la rupture fragile.
Mathematical Methods in Applied Sciences, 3, pp. 70-87.

8. CETIM internal report, "Facteur d'Intensité des Contraintes dans les Piquages Fissurés". Senlis France, 1986.

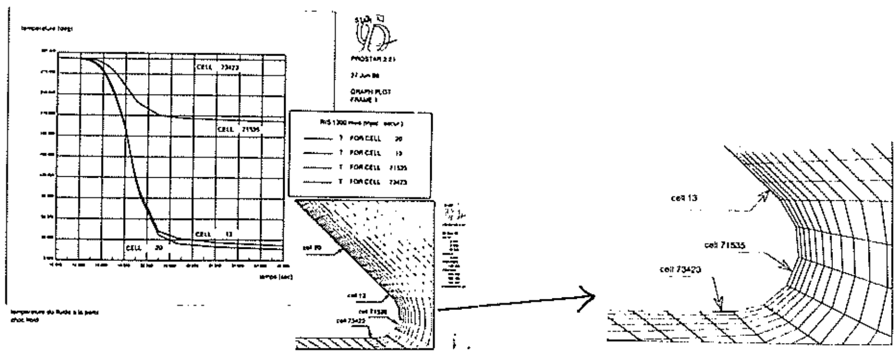

Figure 1: Temperature variation in the fluid close to the corner.

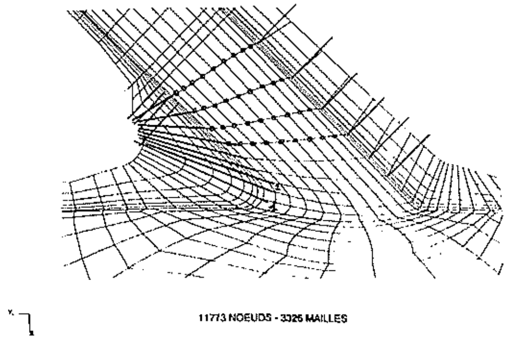

Figure 2 : Some wall cross sections considered in the determination of the crack location.

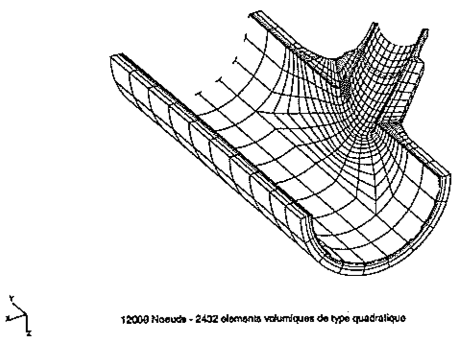

Figure 3 : Mesh automatically generated for mechanical analyses.

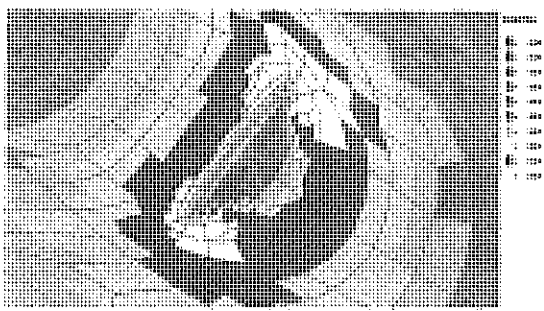

Figure 4 : Isomises around the corner crack under 20.7 MPa.

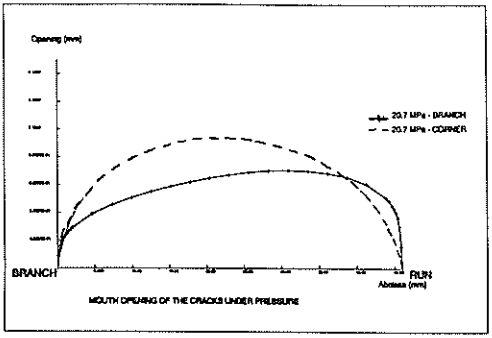

Figure 5a : Run & branch crack openings under pressure.

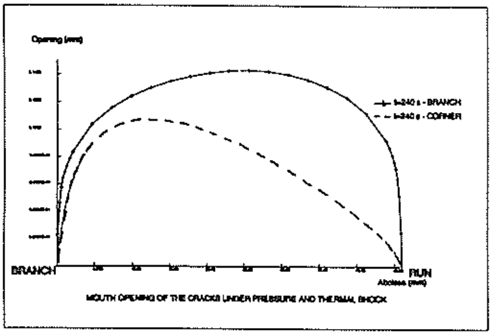

Figure 5b : Run & branch crack openings under constant pressure and thermal shock.

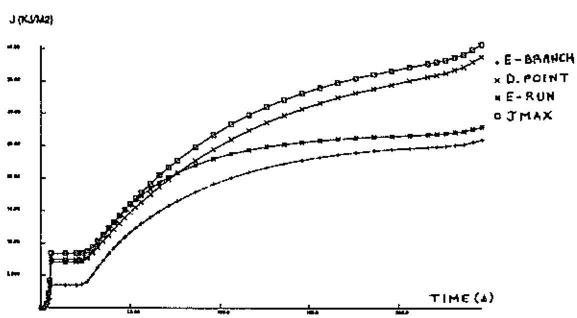

Figure 6 : J variation at several locations along the branch crack.